technische universität
dortmund

Arbeit zur Erlangung des akademischen Grades
Bachelor of Science

Flavour Mixing Effects in the Direct Detection of Dark Matter

Anja Beck
geboren in Kempten (Allgäu)

2017

Lehrstuhl für Theoretische Physik IV
Fakultät Physik
Technische Universität Dortmund

Erstgutachter:	Jun.-Prof. Dr. Joachim Brod
Zweitgutachter:	Prof. Dr. Heinrich Päs
Abgabedatum:	12. Juli 2017

Altmannshofer et al. correctly neglected CKM mixing in their predictions for dark matter direct detection.

Since there are no restrictions concerning the imaginary part of C_{2bs}, we enlarge $\mathrm{Im}(C_{2bs})$ until we reach $\sigma_{0,\mathrm{loop}}$ in Figure 5.3. But this can only be achieved by choosing imaginary parts two orders of magnitude larger than the real part of C_{2bs}. Even though this is possible, we consider an imaginary part of this magnitude to be very odd.

Second, we focus on the relic density condition in equation (4.2). To that end, we set $m_{Z'} = 2m_\chi$, but allow for a 30 % tolerance. For $q_\chi = 1$, we set g' to the lower bound in (4.4): $g' = 2 \cdot 10^{-3}$, and for $q_\chi = 1/6$, we guess $g' = 10^{-2}$. Figure 5.4 shows the corresponding loop cross section again as a green shaded area. Regarding the tree level cross section, we choose C_{2bs} in strong accordance with (5.1). We find that there are regions for m_χ where the tree level cross section reaches the loop cross section. The shaded lines show the lower bound of these regions. At the lower boundary of the green area $m_{Z'} = 2m_\chi \cdot 1.3$. The tables 5.1 and 5.2 show the obtained lower bounds (l. b.) for the dark matter mass, the resulting values for the Z' mass, and the ratio of the Z' mass and the coupling g'. The ratios are clearly far from being within the bounds of equation (4.1) and thus, the region where flavour mixing becomes relevant cannot address the $B \to K\bar{l}l$ discrepancies.

Table 5.1: $q_\chi = 1$. Bounds for dark matter and Z' masses (in GeV) and ratio $m_{Z'}/g'$ (in GeV).

C_{2bs} in GeV^{-2}	l. b. for m_χ	$m_{Z'}$	$m_{Z'}/g'$
$8 \cdot 10^{-10}$	22	57	$29 \cdot 10^3$
$8 \cdot 10^{-10}(1+\mathrm{i})$	18	48	$24 \cdot 10^3$
$3 \cdot 10^{-9}$	11	29	$15 \cdot 10^3$

Table 5.2: $q_\chi = 1/6$. Bounds for dark matter and Z' masses (in GeV) and ratio $m_{Z'}/g'$ (in GeV).

C_{2bs} in GeV^{-2}	l. b. for m_χ	$m_{Z'}$	$m_{Z'}/g'$
$1/6 \cdot 8 \cdot 10^{-10}$	108	281	$28 \cdot 10^3$
$1/6 \cdot 8 \cdot 10^{-10}(1+\mathrm{i})$	91	237	$24 \cdot 10^3$
$1/6 \cdot 3 \cdot 10^{-9}$	56	146	$15 \cdot 10^3$

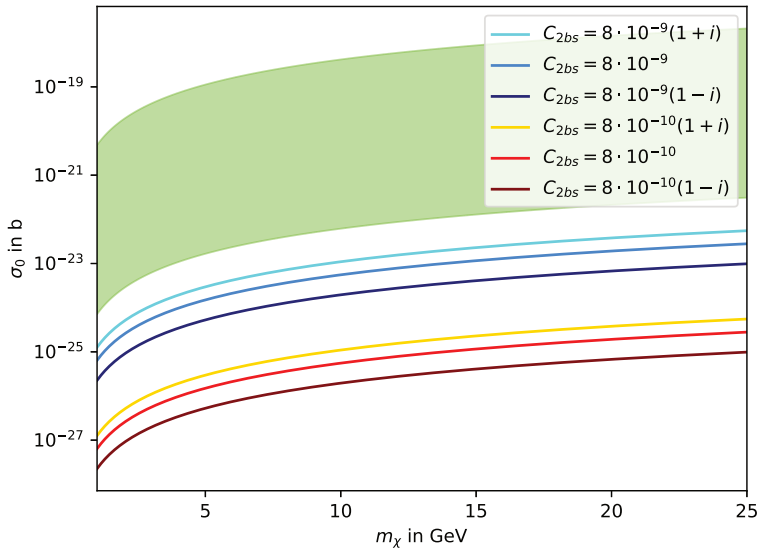

(a) $q_l = q_\chi = 1$

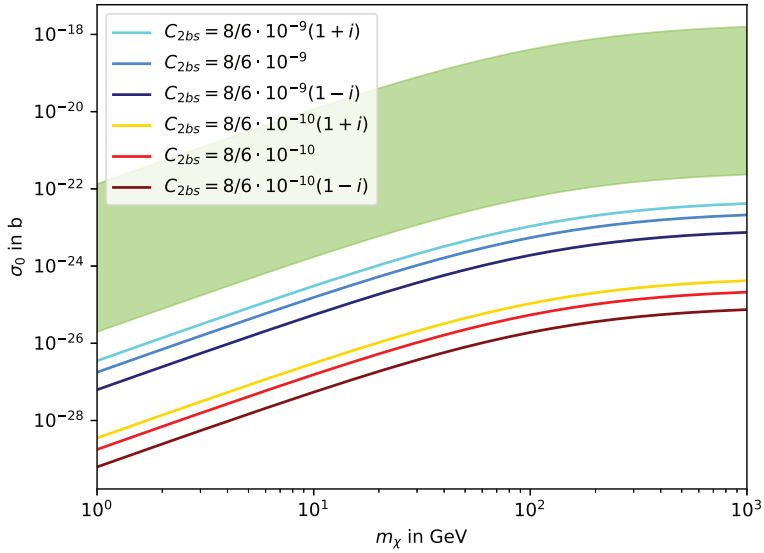

(b) $q_l = 1, q_\chi = 1/6$

Figure 5.2: Comparison of nucleon cross sections with focus on the bound in equation (4.1) that addresses anomalies in $B \to K\bar{l}l$. The shaded green area represents $\sigma_{0,\text{loop}}$ with the bounds in (4.1). The coloured lines show $\sigma_{0,\text{tree}}$ for different values of C_{2bs} (in GeV^{-2}).

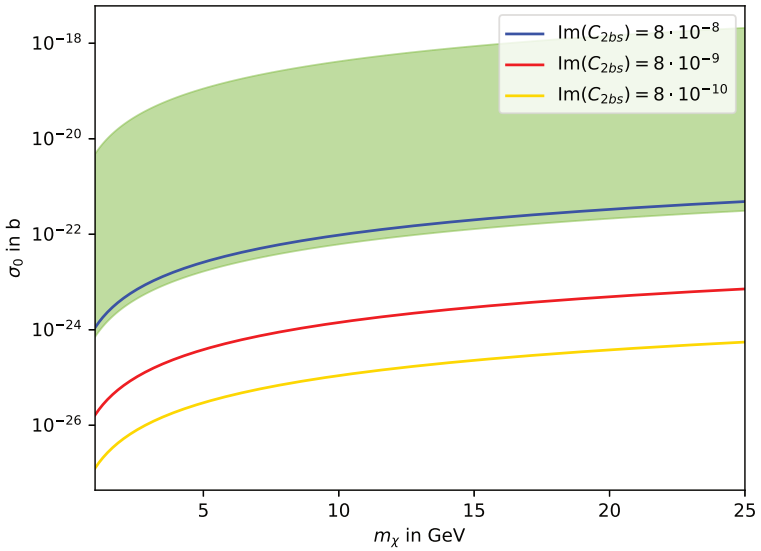

(a) $q_l = q_\chi = 1$

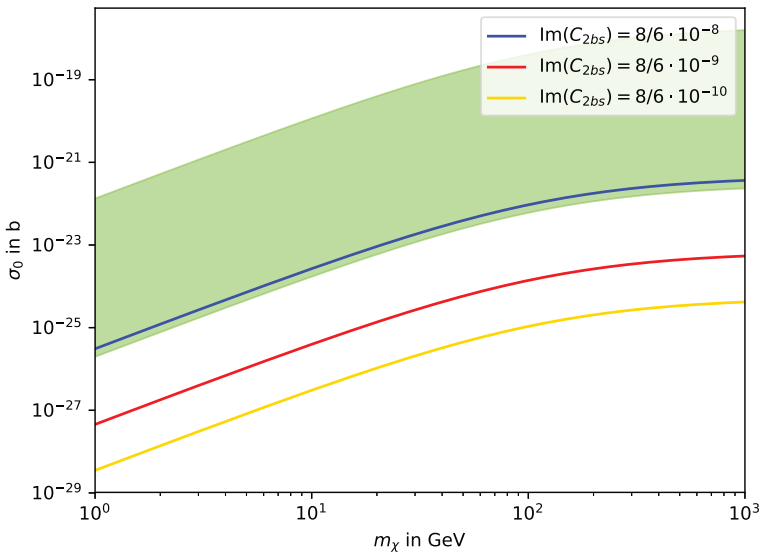

(b) $q_l = 1, q_\chi = 1/6$

Figure 5.3: Like 5.2, but the real part of C_{2bs} is fixed at $8 \cdot 10^{-10}\,\mathrm{GeV}^{-2}$ and only $\mathrm{Im}(C_{2bs})$ is varied.

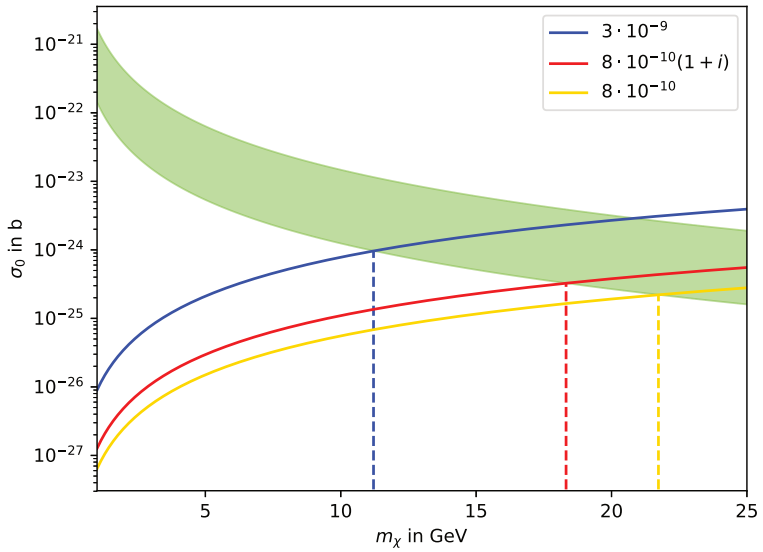

(a) $q_l = q_\chi = 1, g' = 2 \cdot 10^{-3}$

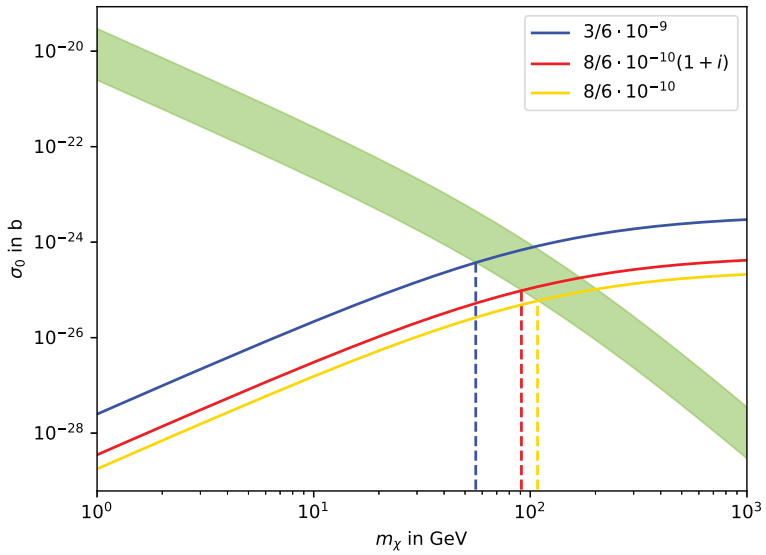

(b) $q_l = 1, q_\chi = 1/6, g' = 10^{-2}$

Figure 5.4: Comparison of nucleon cross sections with focus on the bound in equation (4.2) that produces the right relic density. The shaded green area represents the loop cross section $\sigma_{0,\text{loop}}$ at fixed coupling constant g' and $m_{Z'} = 2m_\chi$ with a $\pm 30\,\%$ tolerance.